



## Modifier-free fabrication of durable and multifunctional superhydrophobic paper with thermostability and anti-microbial property



Gang Wen<sup>a,b</sup>, Xiaoyu Gao<sup>a,b</sup>, Pan Tian<sup>a,b</sup>, Lieshuang Zhong<sup>a,b</sup>, Zelinlan Wang<sup>a,b</sup>, Zhiguang Guo<sup>a,b,\*</sup>

<sup>a</sup> Hubei Collaborative Innovation Centre for Advanced Organic Chemical Materials and Ministry of Education Key Laboratory for the Green Preparation and Application of Functional Materials, Hubei University, Wuhan 430062, People's Republic of China

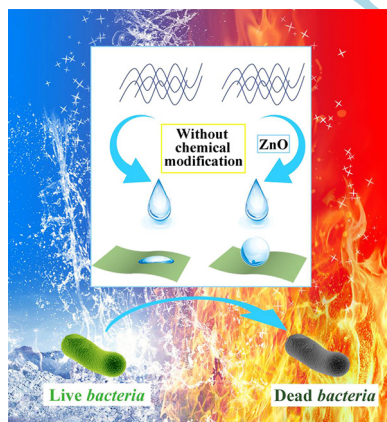
<sup>b</sup> State Key Laboratory of Solid Lubrication, Lanzhou Institute of Chemical Physics, Chinese Academy of Sciences, Lanzhou 730000, People's Republic of China

### HIGHLIGHTS

- Modifier-free fabrication of superhydrophobic and fire-resistant paper.
- The as-prepared paper still remains superhydrophobicity after 500 °C high temperature treatment.
- The as-prepared paper exhibits excellent anti-bacterial property, which has not reported in nonflammable paper.

### GRAPHICAL ABSTRACT

A green and facile method originally is proposed to achieve modifier-free superhydrophobic and fire-resistant paper with excellent anti-bacterial property. Significantly, the paper still remains its superhydrophobicity after being burned and the water repellence will be kept even treatment with 500 °C high temperature. Besides, the specific layered structure will provide high resistance to mechanical destruction.



### ARTICLE INFO

**Keywords:**  
Superhydrophobicity  
Fire-resistance  
Without chemical modification  
Oil adsorption-combustion

### ABSTRACT

The superhydrophobic paper containing CMC, HAP and ZnO was prepared by a novel and facile method with eco-environmental and modifier-free process. The superhydrophobic property is effectively controlled by different amount of ZnO, which might be effect of surface roughness of the paper. Except for the common performances, such as self-cleaning property, chemical durability and mechanical abrasion durability, the excellent thermal stability and anti-bacterial properties will dramatically extend the practical applications of the paper. In addition, such paper still maintains its superhydrophobicity after flammable oil adsorption-combustion, further validating its excellent fire-resistant property. The combination of superhydrophobicity and flame retardancy can largely enhance the durability of the paper. These characteristics make the multifunctional paper a better candidate than the commercial paper, which may be a breakthrough in paper-making industries.

\* Corresponding author at: Hubei Collaborative Innovation Centre for Advanced Organic Chemical Materials and Ministry of Education Key Laboratory for the Green Preparation and Application of Functional Materials, Hubei University, Wuhan 430062, People's Republic of China.

E-mail address: [zguo@licp.cas.cn](mailto:zguo@licp.cas.cn) (Z. Guo).

<https://doi.org/10.1016/j.cej.2018.04.023>

Received 10 February 2018; Received in revised form 20 March 2018; Accepted 5 April 2018

Available online 06 April 2018

1385-8947/ © 2018 Elsevier B.V. All rights reserved.

## 1. Introduction

Paper is a universal and essential material that is available in many fields due to its low cost and scalability [1–3]. However, commercial paper consisting of plant cellulose is easily decomposed and damaged by chemical, physical and thermal treatment [4–7]. Among these, developing materials with tunable surface wettability is one such interesting research direction that expanded to several potential applications [8–11]. Several studies have confirmed that superhydrophobicity is a combination of roughness and low surface energy material [12–14]. To date, researchers have fabricated several artificial superhydrophobic surfaces through two different approaches: preparing a rough surface on hydrophobic materials or modifying a rough surface with low surface energy materials [15]. In general, sophisticated processes such as template [16], etching [17] and plasma treatment [18] are involved in constructing a rough surface, and fluorine-containing low surface energy materials are used to realize superhydrophobicity. However, most low surface energy materials are organic solution, which are usually fragile, required expensive chemicals or longer times and harmful to the environment [19–21]. These drawbacks have great effect on the wide spread practical applications of superhydrophobic surfaces for large-scale production [22]. Therefore, a cost-efficient and straightforward process is more preferable.

Besides, the applications of paper are not limited to water-repellency. Impacting antibacterial property may be crucial for the paper in the fields of medical treatment and food packing, not only to prevent microorganism from being contacted with the surface of paper, but also to restrain the growth of bacteria and further kill the microorganism. In medical treatment, serious damages can result from infection caused by microorganisms especially *Staphylococcus aureus* (*S. aureus*) and *Escherichia coli* (*E. coli*) [23–25]. And anti-bacterial materials have therefore attracted much attention. As broad-spectrum antimicrobial agents, silver nanoparticles (AgNPs), as well as graphene have been incorporated into papers to achieve anti-bacterial property [26,27]. However, antimicrobial agents sometimes are unstable and result in cell toxicity [28]. And the used process also alters the properties of the paper matrix, which may hinder the final product usability for certain applications.

So far, papers with simultaneous superhydrophobic and flame-retardant characteristics appear rarely in the literature. And poor water-proofness and microbial infection potential of the paper, the scope of their use is limited. Among a series of materials, hydroxyapatite ( $\text{Ca}_{10}(\text{OH})_2(\text{PO}_4)_6$ , HAP) with considerable non-toxicity and biocompatibility [29] has been reported by Zhu's group, [30] which performs the obviously advantage of inherent non-flammable property. ZnO with nontoxic, [31] low-cost, anti-bacterial [32] and controlled structure [33] was used in the present work to expand the practical applications of the paper. Herein, a green and facile method originally was proposed to achieve outer and inner uniform and modifier-free superhydrophobic and nonflammable paper with excellent anti-bacterial property. The outstanding performances of superhydrophobic and fire-resistant paper and its absolutely green preparation for scale-up suggest that it has potential applicability in both industries and medical fields.

## 2. Experimental

### 2.1. Materials and chemicals

Calcium chloride ( $\text{CaCl}_2$ ), sodium dihydrogen phosphate ( $\text{NaH}_2\text{PO}_4\cdot\text{H}_2\text{O}$ ), zinc oxide powder ( $\text{ZnO}$ , < 100 nm) was purchased from Guangzhou XILONG Chemical Reagent Co. Ltd, China. Sodium hydroxide ( $\text{NaOH}$ ) was purchased from Tianjin LIANLONGBOHUA Chemical Reagent Co. Ltd, China. Carboxymethyl cellulose (CMC) was purchased from Meryer Chemical Technology Co. Ltd, China. All chemicals were used as received without further purification.

### 2.2. Preparation of HAP nanowires

HAP nanowires were synthesized based on the previous work [30]. Briefly,  $\text{CaCl}_2$  (0.22 g) aqueous solution (20 mL),  $\text{NaOH}$  (1.00 g) aqueous solution (20 mL), and  $\text{NaH}_2\text{PO}_4\cdot\text{H}_2\text{O}$  (0.28 g) aqueous solution (10 mL) were added drop-wise into the mixture containing ethanol (12.00 g) and oleic acid (12.00 g) under vigorous stirring conditions, respectively. And then the mixture was transferred into a 100 mL Teflon-lined steel autoclave. The autoclave was kept at 180 °C for 24 h under standard conditions. After cooling, HAP nanowires were stirred in ethanol and water for 12 h, respectively. Subsequently, the solution was centrifugated and stored in ethanol for the following experiment.

### 2.3. Preparation of paper with different wettability

To enhance the strength, 1 g CMC was dissolved in 100 mL water, forming viscous solution. And 3 mL CMC aqueous solution was added into the ethanol containing HAP nanowires. Different amount of ZnO (0, 0.4, 0.8, 1.2 g, labeled as P – ×g), while the other experimental conditions were kept in the same, was dissolved in deionized water (100 mL), respectively. And 1 mL  $\text{NH}_3\cdot\text{H}_2\text{O}$  was added into the above solution. Under continuous and vigorous stirring for 12 h, the mixture was filtrated using a vacuum pump and dried at 60 °C to obtain white and uniform paper.

### 2.4. Antibacterial test

The antibacterial ability was evaluated by surface plate intuitively. The *E. coli* (a gram-negative bacterium) and *S. aureus* (a gram-positive bacterium) were selected as the model bacteria. All bacteria were cultured in the sterile Luria-Bertain (LB) media (containing 1 g bacto-tryptone, 0.5 g of bacto-yeast extract and 1 g of NaCl in 100 mL of deionized water) at 37 °C, separately. During the antibacterial tests, all the samples, including raw paper and superhydrophobic paper, were sterilized with 75% alcohol and then exposed under ultraviolet radiation for 30 min.

All of the sample were put into 96-well plates and 100  $\mu\text{L}$  of bacterial liquid was added into each well. And the bacterial liquid had been diluted with LB media to  $1 \times 10^5$  colony-forming units (CFU) per milliliter. After the incubation time, 10  $\mu\text{L}$  of bacterial liquid was taken out for dilution with LB media 100 times. Then, 10  $\mu\text{L}$  of diluted bacterial liquid was taken out to be evenly poured into each plate, which included 7 mL of solid LB agar. Finally, the number of bacterial colonies on the surface of raw paper and superhydrophobic paper and the number of residual bacterial colonies on surface plates were photographed and counted by digital photo after culturing for 1 day at 37 °C.

### 2.5. Characterization

The crystal structure was characterized by X-ray diffraction (XRD) using an X'PERT PRO diffractometer with Cu K $\alpha$  radiation of 1.5418 Å wavelength at  $2\theta$  ranging from 5° to 120°. Field emission scanning electron microscope (FESEM) images was obtained on JSM-6701F with Au-sputtered specimens. Three-dimensional surface imaging of the paper was carried out using Surface Imaging System atomic force microscopy (AFM, CSPM 5500). The element distribution maps of samples were got by energy dispersive spectroscopy (EDS, Kevex). Fourier transform infrared spectroscopy (FTIR, Thermo Scientific Nicolet iS10) was recorded as KBr disks on a Bruker 1600 FTIR spectrometer. The water contact angle (WCA) was measured with a DSA 100 contact angle meter (Kruss Company, Germany) or JC2000D with 5  $\mu\text{L}$  distilled water droplet at ambient temperature. The average WCA values were obtained by measuring the same sample at five different sites. Thermal gravimetric analyses (TGA) was performed on a NETZSCH STA 449C using a dynamic heating rate of 10 °C  $\text{min}^{-1}$  under an atmosphere of air. All photographs were taken using a Sony camera (DSCHX200).

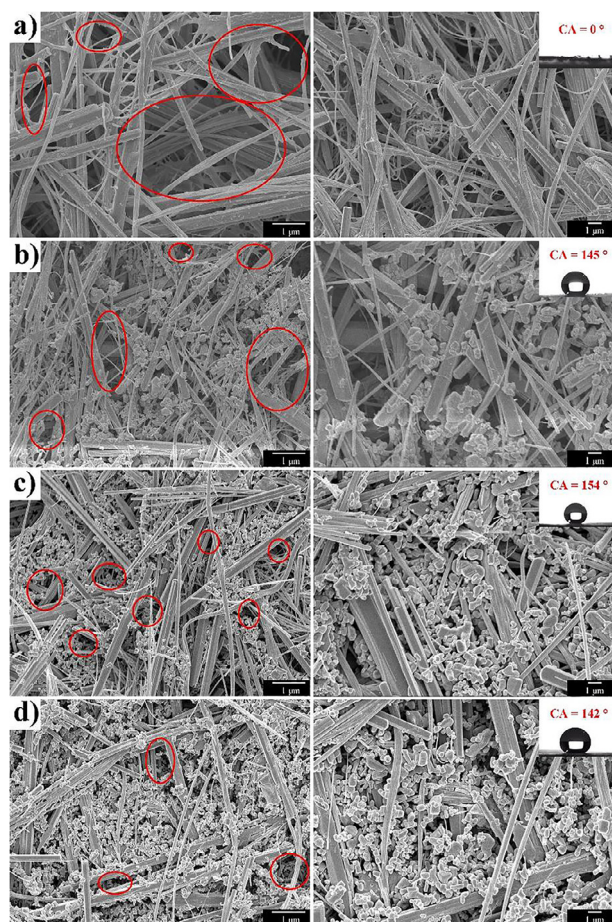


Fig. 1. SEM images of a) raw paper, b) P – 0.4, c) P – 0.8, d) P – 1.2. The corresponding optical photographs of water droplet are shown in the inset. Marked region represents the variation of intensity and size of the air pockets.

### 3. Results and discussion

#### 3.1. Surface preparation, wettability and morphology

The relationship between ZnO loading and water contact angle (WCA) on the hydrophobic property of the paper was shown in Fig. S1. The amount of ZnO in the system was optimized as an essential function of the WCA. Apparently, the WCA value of paper increased with the increasing amount of ZnO. And the WCA value of paper increased from  $0^\circ$  to  $154^\circ$  when the ZnO loading reached to 0.8 g, indicating that the ZnO loading greatly influenced the wettability within the limits. However, further increasing the ZnO loading, the wettability has changed greatly, possible due to the change in the surface roughness. The maximum WCA of  $154^\circ$  can be achieved at ZnO loading of 0.8 g. To explain the variation of WCA with ZnO loading, SEM images with different ZnO loading were shown in Fig. 1a–d. Obviously, the surface of raw HAP nanowires was relatively smooth, whereas the morphologies of HAP nanowires with different ZnO loading were hierarchical micro- and nanostructure. To check the aforementioned observation, the roughness of the paper was measured. The three-dimensional AFM images of papers for different ZnO loading were shown in Fig. 2. For the raw paper without ZnO, it was obvious that it completely consisted of HAP nanowires and exhibited a relatively flat topography with an average surface roughness ( $R_a$ ) of about 102 nm. Furthermore, the  $R_a$  values for 0.4, 0.8 and 1.2 g ZnO loading were 148, 182 and 208 nm, respectively. In general, the surface roughness is a determined factor for the fabrication of superhydrophobic surface. However, the maximum WCA was corresponded to the average surface roughness of 182 nm

instead of 208 nm, which is not consistent with the experimental results. Based on the above mentioned results, the detail explanations were as followed: Firstly, although there was no chemical modification with low surface energy materials, the anisotropic preferred growth plane of ZnO possessed lower surface free energy [34]. Thus, the existence of ZnO and micro- and nanostructure could make it possible for the superhydrophobicity without chemical modification. Subsequently, the maximum WCA was theoretically resulted from the  $R_a$  of 208 nm. Therefore, we could boldly speculate that the surface roughness was not determined by an individual factor of ZnO nanoparticles or HAP nanowires, it was caused by the combination of aforementioned factors. When the ZnO loading was ranged from 0 to 0.8 g, the surface roughness made from HAP nanowires and ZnO nanoparticles resulted in the increase of WCA. Tubercles consisting of overmuch agglomerate ZnO nanoparticles on the surface were resulted from the increasingly ZnO loading (1.2 g). In this case, the factor of ZnO nanoparticles played a dominate role in determining surface roughness and the effect of hierarchical structure was weakened, contributing to the reduction of WCA. In deeper level, the increase of the density and fraction of air pockets (highlighted in red in Fig. 1) and a large fraction of air within the grooves trapped by the combination of HAP nanowires and ZnO nanoparticles also could be explained the superhydrophobicity of paper.

To further confirm that ZnO nanoparticles were successfully deposited on the surface of HAP nanowires, the characterizations of XRD, XPS and EDS were conducted. In order to investigate the influence of ZnO on the crystalline phase of the paper, XRD measurements of pure ZnO (JCPDS No. 36-1451), raw HAP paper (JCPDS No. 74-0565) and superhydrophobic paper were presented in Fig. 3a. It was clear that all of the diffraction peaks of superhydrophobic paper except for the characteristic peaks of the raw paper can be indexed to ZnO. Besides, from the result of XPS, Ca, O, P, C and Zn elements could be obviously observed in superhydrophobic paper. Compared with the raw paper, Fig. 3c reveals that the obvious Zn 2p appeared after adding ZnO. This is confirmed that ZnO is well bound to the HAP nanowires. The analysis of surface elements is a necessary means to directly prove the changes of the surface chemical composition. EDS analysis (Figs. 3d and S2) was carried out to investigate the chemical composition of the paper. There are only Ca, O, P, C elements in the raw paper. To further confirm the distribution level, elemental analysis of the superhydrophobic paper was performed. It was found that Zn element uniformly distributed in the surface of paper. These results indicated that ZnO nanoparticles were successfully deposited on the surface of HAP. Besides, the FTIR of raw paper and superhydrophobic paper were presented in Fig. 3b. Several characteristic absorption peaks were observed in the range  $460\text{--}4000\text{ cm}^{-1}$ . The absorption bands observed at  $3565\text{ cm}^{-1}$  and  $633\text{ cm}^{-1}$  are attributed to hydroxyl group [35]. Moreover, there exist the adsorption peaks of the  $\text{PO}_4^{3-}$  group ( $1093, 1028, 962, 604, 561\text{ cm}^{-1}$ ) [36]. The adsorption peaks at  $2921\text{ cm}^{-1}$  and  $2852\text{ cm}^{-1}$  are attributed to the stretching vibrations of C–H in  $-\text{CH}_3$  and  $-\text{CH}_2-$  groups of oleic acid [37]. It was noted that the adsorption peaks at  $478\text{ cm}^{-1}$  was attributed to the stretching vibration of Zn–O bond. The abovementioned results demonstrated ZnO nanoparticles were successfully deposited on the surface of HAP nanowires.

In order to enhance the strength of paper, carboxymethyl cellulose (CMC) was cooperated into HAP nanowires, (Fig. S3b) whereas the strength of raw paper was so poor that the raw paper was easy to be broken (Fig. S3a). And the strength of paper increases with the increasing concentration of CMC. However, HAP nanowires solution containing of redundant CMC would come into being viscous solution, making it difficult for filtration process of paper. Therefore, an appropriate concentration of CMC was thus confirmed to prepare paper. Fig. S4 shows a sheet of superhydrophobic HAP nanowires paper with about 3.90 cm in diameter, 0.48 mm in thickness and 0.65 g in weight. The water contact angle is  $154^\circ$  and sliding angle is about  $5^\circ$  (Fig. 4b). In addition, just as shown in Fig. 4c, the superhydrophobic paper

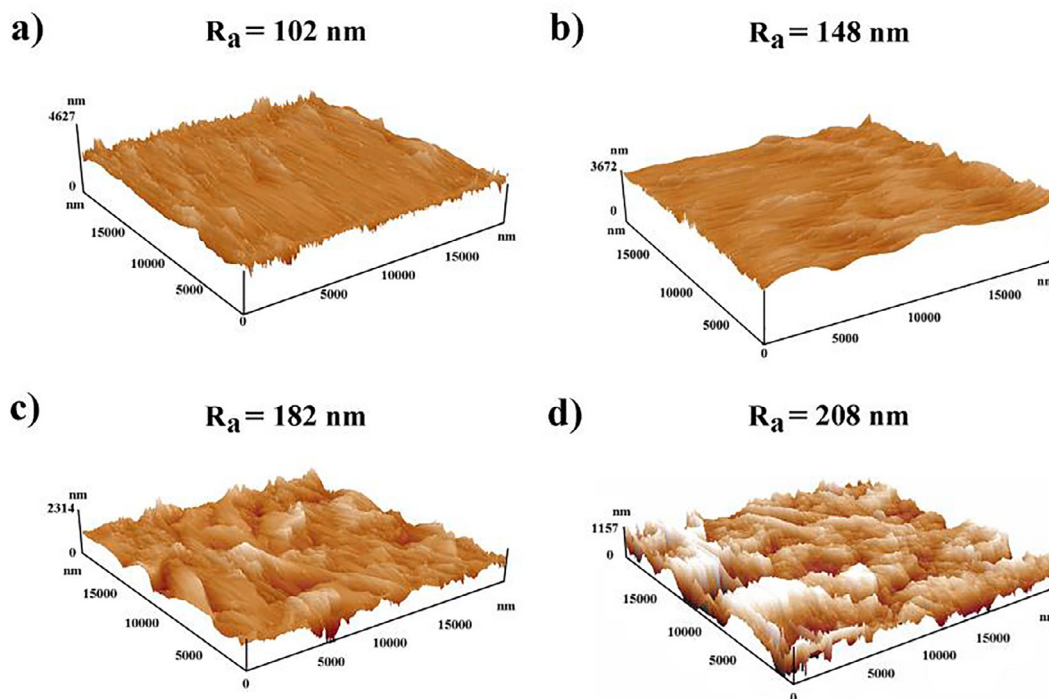


Fig. 2. AFM images of a) raw paper, b) P = 0.4, c) P = 0.8, d) P = 1.2.

exhibited great antiwetting performance towards to some common liquids, such as tea, coffee and milk. Furthermore, it could be observed that the droplets with pH = 3 and pH = 12 maintained the spherical shape on the surface of superhydrophobic paper, indicating the acid-alkali tolerance of superhydrophobic paper.

### 3.2. Self-cleaning and anti-wetting properties

The self-cleaning property, as one of the most important factor to measure the characterisation of superhydrophobicity, is an effective tool to prevent paper from being contaminated by solid dirt in the presence of water [38–40]. And self-cleaning is a desired property that can make the dream of a contamination-free surface come true. The self-cleaning measurement was further conducted using sand as a

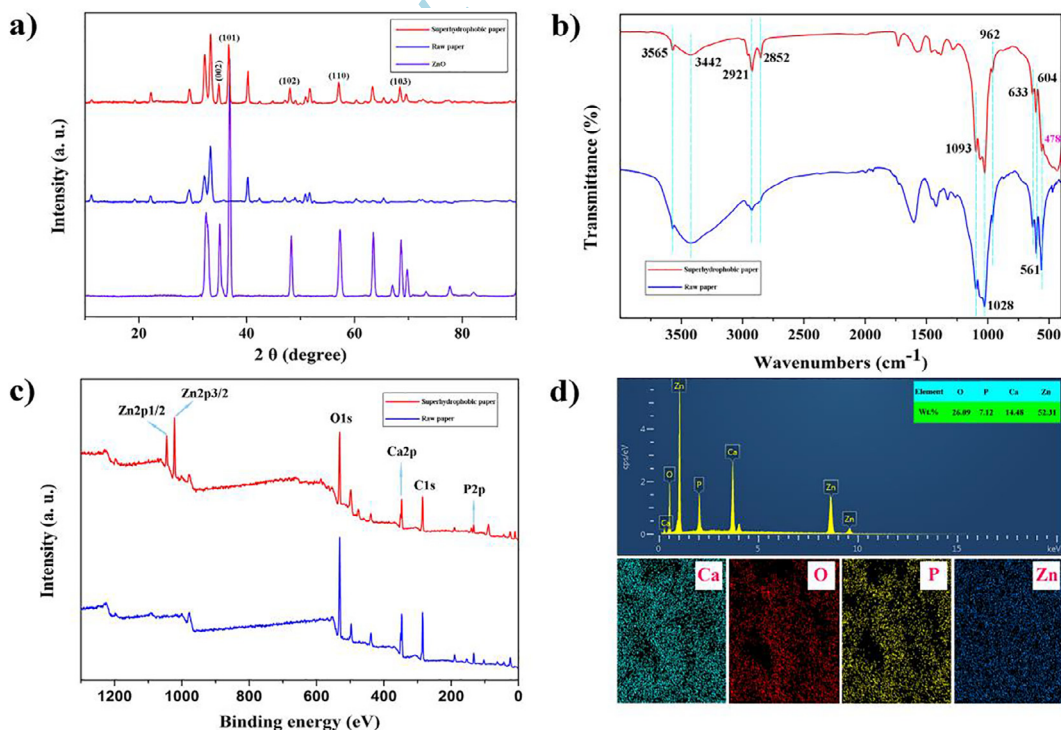


Fig. 3. a) XRD patterns of raw paper, superhydrophobic paper. b) The FTIR spectrum of raw paper and superhydrophobic paper. c) The XPS spectra of raw paper and superhydrophobic paper. d) EDS spectra and FESEM-EDS mapping of superhydrophobic paper.

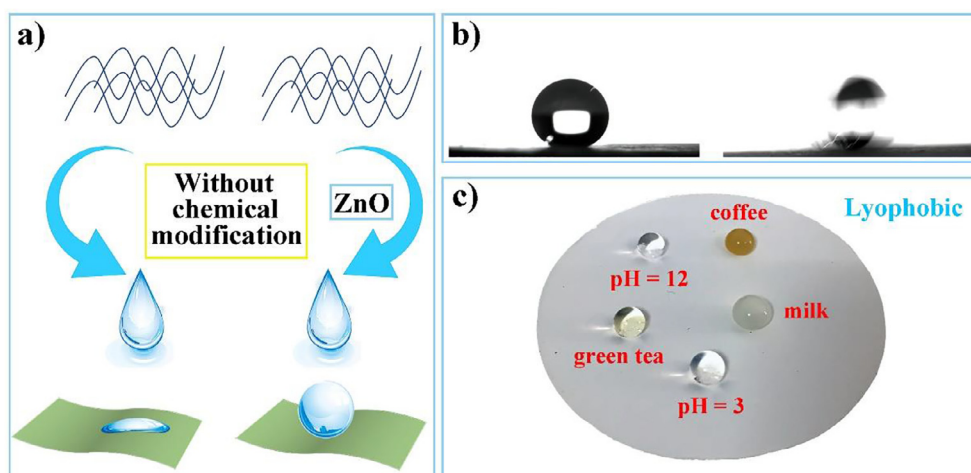


Fig. 4. a) Schematic illustration of superhydrophobic paper without chemical modification. b) Pictures of water contact angle and water droplet (5  $\mu$ L) sliding off a 5° tilted superhydrophobic paper surface. c) A lyophobic property photograph of the superhydrophobic paper toward daily liquids such as coffee, milk, green tea, water with pH = 3, and water with pH = 12.

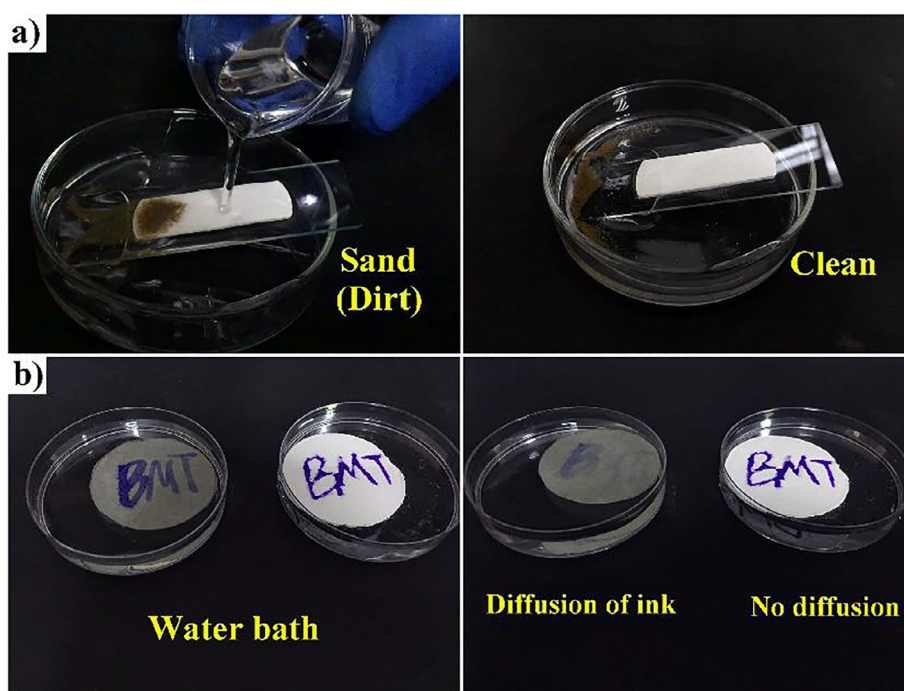
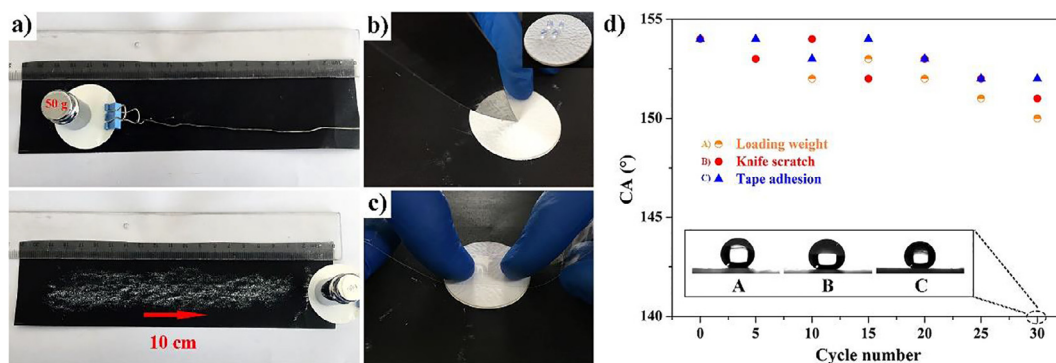


Fig. 5. a) Self-cleaning property of the superhydrophobic paper. b) Ink on the normal paper diffused as it came in contact with water, whereas it remained intact on superhydrophobic paper.

contaminant. Obviously, the sand could be easily carried from the paper surface, demonstrating the self-cleaning phenomenon was obviously found towards the dust. (Fig. 5a) While hydrophilic in nature, raw paper can be easily wetted through the diffusion (capillary action) of water, affecting the integrity of the raw paper. In order to demonstrate waterproof ability of superhydrophobic paper, raw paper and superhydrophobic paper were tested with ink diffusion, where both the papers were written with water-diffusile blue ink and exposed to a water bath at the same time. (Fig. 5b) It was noted that the blue word “BMT” was made up of a large number of dense droplets. Within a few minutes, raw paper became wet and the blue word “BMT” of the surface was diffused during the experiment. On the contrary, the word on superhydrophobic paper remained unchanged and no water droplets were immersed into the other side of the paper. This kind of excellent property will enhance the usability of such paper in paper-based industries.

### 3.3. Chemical and environmental durability

For practical applications, superhydrophobic materials are urgently required to retain their inherent performances under different extreme conditions [41]. Therefore, we conducted the common solvents, UV, acid, alkali solutions and boiling water resistances to measure the stability of superhydrophobic paper [42,43]. The as-prepared superhydrophobic paper was immersed in organic solvents, such as acetone, ethanol and DMF for 24 h. After it was dried, the variations of corresponding water contact angles and sliding angles were measure (Fig. S5a-c). After immersed in acetone, the WCAs and CAs of superhydrophobic paper performed barely change. The WCAs changed from 153° to 150° and the SAs decreased from 5° to 8°, validating the solvent resistance of superhydrophobic paper. Similarly, when immersed in ethanol and DMF, the water repellence of superhydrophobic paper maintained unchanged. The considerable solvent resistance of the superhydrophobic paper can be attributed to the air layer on the surface of superhydrophobic paper. Therefore, the superhydrophobic paper



**Fig. 6.** Mechanical damages induced on superhydrophobic paper. a) sand paper abrasion with 50 g of load. b) Scratching with a knife. c) Tape adhesion test. d) Durability test for the superhydrophobic paper. Variation in WCA of water droplet during multiple abrasion cycles. One experiment consists of 5 complete abrasion cycles. (Inset) Photograph showing static contact angle of water on mechanically tested surfaces (after the 30th cycle).

could make it possible for antifouling even when encountering organic liquids, superior to the lotus leaf. Besides, UV-durability test conducted by irradiation using an artificial light as the source of radiation. The superhydrophobic paper was exposed to UV light for 24 h and the wetting behavior was measured every 4 h. Just shown in Fig. S5d, the CA changed slightly and the corresponding SA was lower than  $10^\circ$  after 24 h UV radiation. Under UV irradiation, the hydrophobicity has a tendency to decrease as a function of irradiation time. The reason why the WCA decreases slightly can be explained by the frame of creation of oxygen vacancies of a small amount of ZnO on the surface of superhydrophobic paper [44]. Electron-hole pairs are generated in their lattice when the surface of these oxides is illuminated by UV light [45,46]. Some of the holes react with the lattice oxygen, forming oxygen vacancies of the surface of paper, as described in Eqs. 1.11.3.



where  $\square$  is the oxygen vacancy.

In the meanwhile, water may be adsorbed on these oxygen vacancies, resulting in the decrease of WCA.

Another challenge in the practical application is the chemical stability of the superhydrophobic paper. To explore the durability of the superhydrophobicity of the as-prepared paper, the effect of different pH values was examined. As shown in Fig. S5, the as-prepared superhydrophobic paper was immersed into the corrosive solution with different pH values for 1 h to evaluate their WCAs. Changing the pH values from acid (pH = 3) to strong alkali (pH = 12), the measured WCAs were all above  $150^\circ$ . On the one hand, such excellent repellency to corrosive solution was attributed to the micro- and nanoscale structure. As numerous air was trapped within the micro- and nanostructure, the formed dual-scaled air pockets prevented the infiltration of corrosive solution. On the other hand, based on the chemical nature of HAP and ZnO, theoretically, the paper cannot tolerate acid solution at all. The abnormal experimental phenomena may be explained by the theory of precipitation and dissolution equilibrium [47]. When  $\text{pH} \geq 3$ , the concentration of  $\text{H}^+$  is not enough to dissolve the HAP and ZnO, which is coincidence with the well-preserved HAP and ZnO (Fig. S6c). However, when  $\text{pH} = 2$ , it was obvious that the ZnO nanoparticles and HAP nanowires were in the state of being dissolved, affecting its wetting ability. Furthermore, when  $\text{pH} = 1$ , ZnO nanoparticles had been dissolved absolutely and it was hard to recognise the HAP nanowires (Fig. S6a and S6b). Therefore, the water contact angles were  $28^\circ$  and  $125^\circ$ , corresponding to  $\text{pH} = 1$  and  $\text{pH} = 2$ , respectively. In addition, most superhydrophobic paper loses its water repellence property when faced with boiling water and the hot water repellency of a superhydrophobic

surface plays a critical role in the design of highly efficient heat transfer systems. Thus, we tried to conduct the boiling water resistance experiment to explore its property. What astonished us most was that water droplet still could maintain its spherical shape after taking the paper out of the boiling water. The variation of WCAs of superhydrophobic paper for different boiling time was presented in Fig. S5f. The unique network structure can trap lots of air pockets and can ensure air pockets being a stable state, which is responsible for the boiling water resistance of superhydrophobic paper.

#### 3.4. Mechanical abrasion durability

In general, roughness of superhydrophobic surface is relatively weak and easy to be destroyed [48–50]. But the as-prepared paper is a specific layered structure and the superhydrophobicity performs on every layer. To investigate the abovementioned illustration, ruggedness of superhydrophobic paper was studied through serve mechanism abrasion tests, such as sand paper abrasion, knife scratch and tape adhesion. As for sand paper abrasion, the paper was placed on the sandpaper (400 Cw) and loaded with 50 g weight, dragging by steel wire for the length of 10 cm (Fig. 6a). The aforementioned abrasion process was defined as one abrasion cycle. The corresponding WCA with each five abrasion cycles was recorded and presented in Fig. 6d. Obviously, the WCA decreased slightly and the superhydrophobicity of as-prepared paper still remained even after 30 abrasion cycles. The SEM images before and after abrasion test were shown in Fig. S7. From the pictures, we could see that the cross-sectional view of SEM image was a specific layered structure (Figs. S7a and 7c), which ensured the superhydrophobicity of each layer. Moreover, no obvious change could be observed in SEM images, indicating the excellent mechanism durability of superhydrophobic paper (Fig. S7b and S7d). Similar mechanical robustness of superhydrophobicity was also observed in knife scratch and tape adhesion tests. Just as shown in Fig. 6b, after the knife scratch, the water droplets still maintained their spherical shape on the surface. In addition, the as-prepared paper was also subjected to peel off test to investigate the internal superhydrophobicity (Fig. 6c). It could be concluded that even after 30 peeling tests, the paper still maintained its initial superhydrophobic property, which further confirmed the outer and inner superhydrophobicity of the paper. The abovementioned mechanism damage demonstrated that the as-prepared paper performs excellent mechanism durability and water droplets still roll off through the damaged areas, which was benefited from the layered structure.

#### 3.5. Thermal stability and flame retardancy

Generally speaking, almost all of the paper-based materials are unable to be subjected to fire and water simultaneously and the destructive process is devastating and nonrecoverable [51–53]. There is

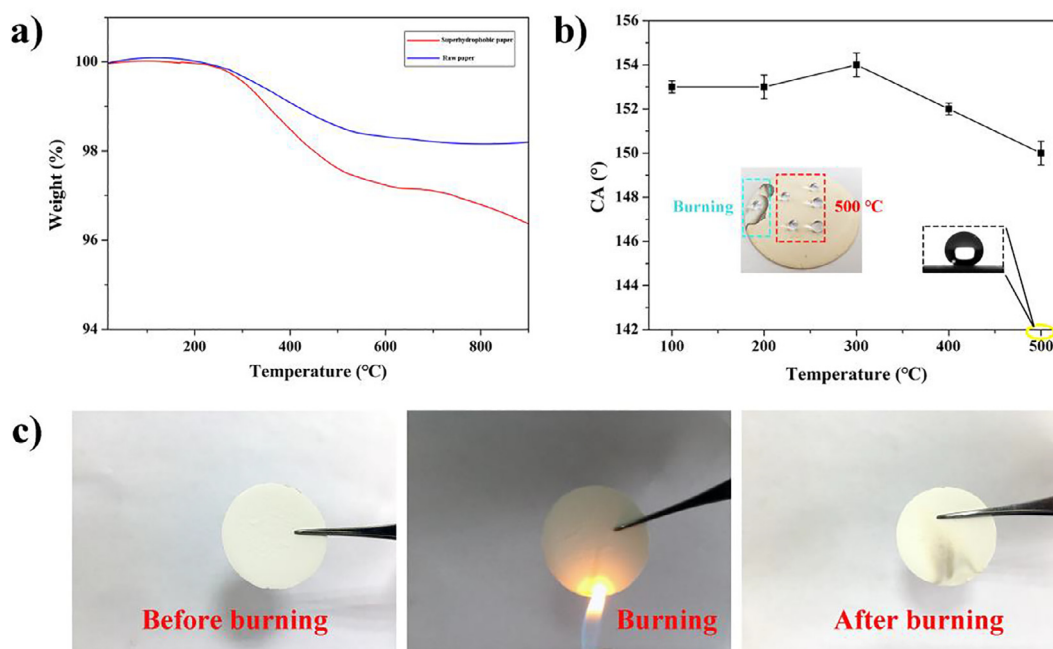


Fig. 7. a) Variation of WCA of the superhydrophobic and fire-resistant paper at 100 °C, 200 °C, 300 °C, 400 °C and 500 °C b) TGA of raw paper and superhydrophobic paper. c) The combustion process of superhydrophobic & fire-resistant paper.

an old saying in China: “be incompatible as fire and water”. Therefore, it is essential to fabricate functional paper that processes both water-proof and nonflammable performances. The as-prepared paper consisting of HAP nanowires and ZnO nanoparticles is a perfect superhydrophobic and fire-resistant material. In order to validate the thermal stability of paper, the TGA curves of raw paper and superhydrophobic paper were analyzed in an air atmosphere. As shown in Fig. 7a, it was noted that the oleate group starts to decompose at about 200 °C. And obvious initial weight loss of superhydrophobic paper in the range of 240 °C–500 °C is attributed to the decomposition of CMC. Furthermore, the superhydrophobic paper was relatively stable when the temperature reached to 900 °C and the weight percentage of residue of superhydrophobic paper was more than 96%, which was similar to raw paper.

On the one hand, in order to explore the variation of wettability at different temperature, WCAs of the superhydrophobic and non-flammable paper at 100 °C, 200 °C, 300 °C, 400 °C and 500 °C after cooled were recorded and presented in Fig. 7b. The water contact angle was about 150° even after treatment at 500 °C, revealing the extreme high-temperature resistance. The superior stability of the superhydrophobic surface was achieved if the roughness and structure of the surface were not damaged after the heat treatment. In order to demonstrate the aforementioned points, SEM images and AFM images of superhydrophobic paper with 300 °C and 500 °C are presented. From Fig. S8, the structures consisting of HAP nanowires and ZnO remained unchanged when treated with 300 °C and 500 °C, separately. In the meanwhile, the corresponding roughness (182 nm or 180 nm) after heat treatment was similar to roughness (182 nm) of the superhydrophobic paper before heat treatment. On the other hand, the combustion process of superhydrophobic and fire-resistant paper was shown in Fig. 7c. After burning, as expected, no obvious change could be observed. The flame on the superhydrophobic paper was weak and extinguished within three seconds, leaving behind a black residue. Moreover, the water droplets still maintained its sphere shape in the burned areas (inset in Fig. 7b), further confirming the good flame-retardant property of the superhydrophobic paper. From the SEM images and EDS spectra of superhydrophobic paper after being burned, it was obvious that the structure remained unchanged and Zn, Ca, O and P elements are still distributed homogeneously on the surface of superhydrophobic paper,

indicating uniform coverage of ZnO on the HAP nanowires surface (Fig. S9). The thermal stability can be significantly attributed to the inherent fire-resistance of HAP nanowires and thermal stability of ZnO. In addition, few literatures have reported such high temperature resistant paper-based material.

### 3.6. Oil adsorption-combustion

Its three-dimensional network structure, superhydrophobicity and fire-resistance make the paper a perfect candidate for the quick remove of flammable organic oils. The superhydrophobic paper exhibited the excellent absorption capacities towards organic oil. When superhydrophobic paper contacted the floating octane (dyed with Sudan red IV for a clear observation) on paper, the octane can be absorbed completely in just 10 s (Fig. 8a). Meaningfully, the recyclability of adsorbent and collection of organic oil are of great significance in oil adsorption. For value solvents, collection by squeezing is a simple way. Yet, this method is not applicable for paper-based materials. Thus, combustion may be an ideal choice and the paper containing of flammable oil was burned (Fig. 8b). It was noted that the paper restored its original color and the superhydrophobicity of the paper had not lost completely. The variations of WCA and SA of the superhydrophobic and fire-resistant paper after oil adsorption and combustion experiment were presented in Fig. 8d. The result indicated that oil adsorption and combustion had no effect on the wettability of the paper. The water droplets still stood on the surface of burned paper even after 30 cycles. Simultaneously, it was seen that no change of the structure and chemicals could be discovered in the SEM image after 30 cycles. (Figs. 8c, S10) The interlaced HAP nanowires and agglomerate ZnO nanoparticles were observed, validating that the integrity of the structure was determined. These performances may further extend the application of paper-based materials, thus making it a promising candidate for the oil-adsorption and combustion.

### 3.7. Anti-bacterial property

Nowadays, problems associated with nonspecific protein adsorption and microbial adsorption on surfaces have become considerable, and the development of anti-bioadhesive surfaces remains a meaningful and

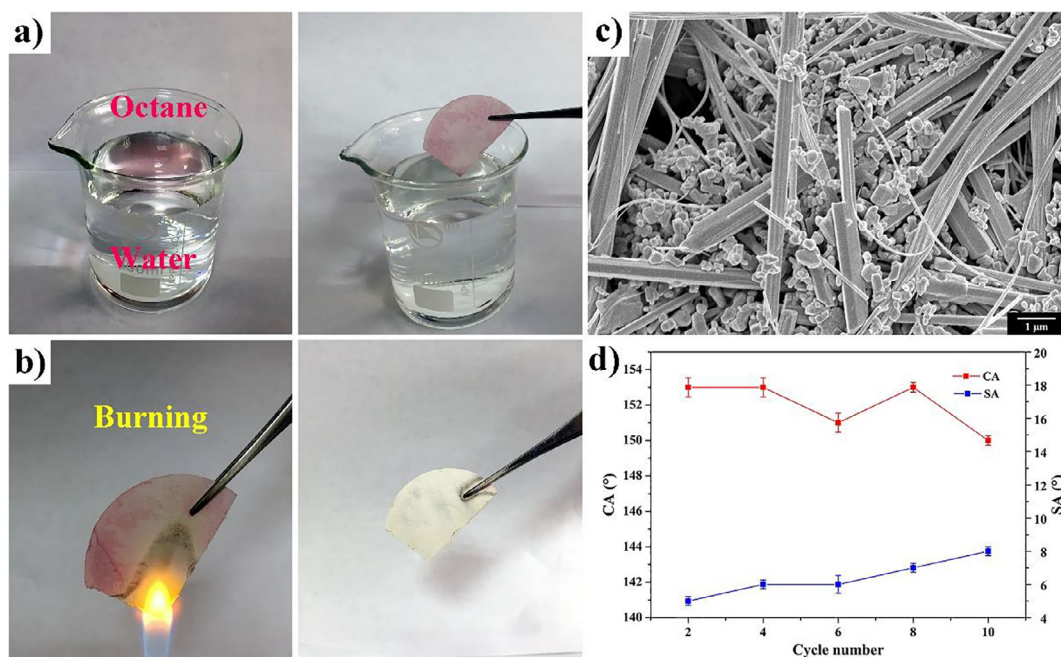


**Fig. 8.** a) Optical images of superhydrophobic paper in oil adsorption experiment (n-octane was dyed by Sudan red IV for a clear observation). b) Optical images of octane-containing superhydrophobic and fire-resistant paper after being burned. c) SEM image of superhydrophobic and fire-resistant paper after the oil-containing paper was burned. d) Variation of WCA and SA of the superhydrophobic and fire-resistant paper after oil adsorption and combustion experiment. One experiment consists of 2 complete cycles. The corresponding optical photographs of water droplet are shown in the inset.

practical goal for application in marine hulls, medical science, and optical surfaces. But in reality, only a few studies have been performed on the application of anti-bacterial to superhydrophobic paper [54–56]. Notably, the effects of surface topography and chemical composition in anti-bacterial are still not clearly understood. Generally speaking, a common strategy to reduce protein fouling is to attach hydrophilic or zwitterionic synthetic polymers to surfaces.

*E. coli* and *S. aureus* are two types of bacteria that are presented in our daily lives. It is known that superhydrophobic surface can reduce the infections by restraining the *E. coli* and *S. aureus* adherence. In order to validate the abovementioned fact and estimate the attachment of the bacterial cells to the surface of the raw paper and superhydrophobic paper, the antibacterial activities of raw paper and superhydrophobic paper through surface plate were presented by performance of microbiological tests against the *E. coli* and *S. aureus* microorganisms. After treated with 24 h, no bacterial community could be observed both on the surface of superhydrophobic paper (Fig. 9b and h) and surface plate (Fig. 9c and i) after vitro antibacterial assay, indicating that the superhydrophobic paper prevented the bacteria from being adhered on the surface and ZnO nanoparticles could effectively kill the bacteria on the surface plate. On the contrary, the bacterial colonies on the surface of raw paper showed little difference with the initial surface plate containing *E. coli* and *S. aureus*. The bacteria still alive when immersed raw paper into the surface plate containing *E. coli* and *S. aureus* for 24 h, separately (Fig. 9f and l) And the residual bacteria on the raw paper was clearly visible (Fig. 9e and k). These results shown that raw paper did not exhibit any antibacterial activity, adequately demonstrating that ZnO played a decisive role in vitro antibacterial assay. The toxic effect of ZnO on microorganisms can be associated with the release of Zinc ions causing disruption of the cell membrane activity and the formation of intercellular reactive oxygen species, mostly  $H_2O_2$ . Therefore, the anti-bacterial activity of ZnO was attributed to the generation of hydrogen peroxide from the surface of ZnO, which was considered to be effective for the inhibition of bacterial growth [57]. The as-prepared superhydrophobic and antibacterial paper can be applied in biomedical field.

#### 4. Conclusion

In summary, the superhydrophobic paper with specific layered network structure, prepared by a facile, modifier-free and green method, under the optimum conditions performs superhydrophobicity and excellent fire-resistance. The water contact angle reaches a maximum value of  $154^\circ$  at the ZnO loading of 0.8 g, and further increase or decrease the ZnO loading will result in the reduction of water contact angle. Although the roughness of surface has influence on the wettability, the redundant hydrophilic ZnO will result in decrease of water contact angle. This is attributed to a combination of an ideal density of air pockets and solid regions made by interlaced HAP nanowires and ZnO nanoparticles. This kind of functional paper with superhydrophobicity, excellent fire resistance, robust durability (against serve mechanism abrasion, boiling water and chemical durability), perfect recyclability and anti-bacterial property is fabricated in the end. It is noted that the superhydrophobic paper possesses oil/water separation ability and the oil is able to be burned. The structure still maintains integrity due to its intrinsic fire-resistant nature and considerable thermal stability. Significantly, the paper is still superhydrophobic after being burned and the water repellence will be kept even treatment with  $500^\circ C$  high temperature. Simultaneously, the specific layered structure will provide high resistance to mechanical destruction. This kind of functional paper may be a breakthrough for paper-based materials, which may subvert the whole paper-making industries. Moreover, the approaches are green and the chemicals involved are inexpensive and environmental friendly as it can be applied to large-scale production.

#### Acknowledgements

This work is supported by the National Nature Science Foundation of China (NO 51522510, 51675513 and 51735013).

#### Appendix A. Supplementary data

Supplementary data associated with this article can be found, in the

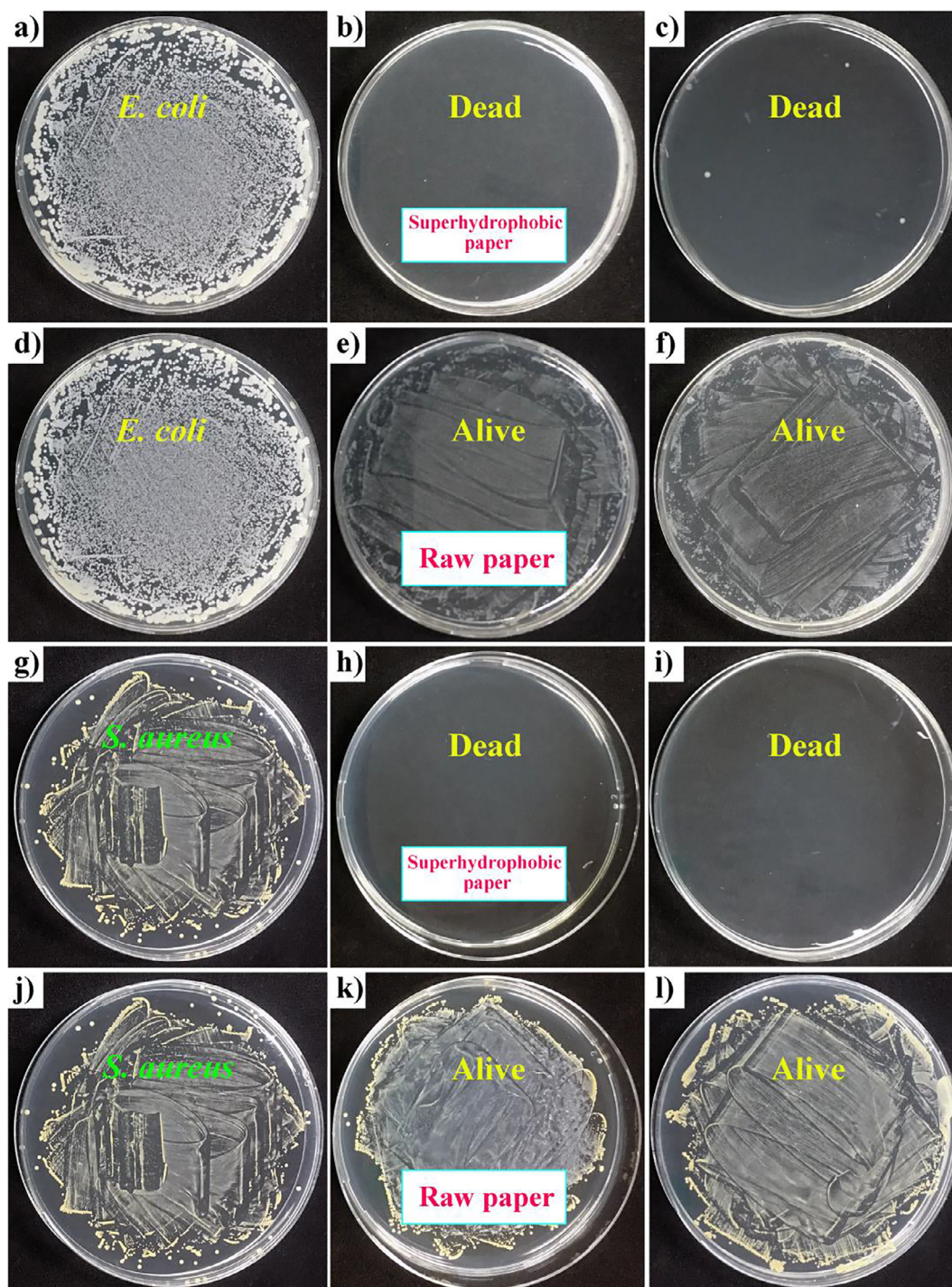


**Fig. 9.** The surface plate of a) and d) *E. coli*. b) The residual amount of bacterial on the superhydrophobic paper. c) The residual amount of bacterial on the surface plate after vitro antibacterial assay. e) The residual amount of bacterial on the raw paper. f) The residual amount of bacterial on the surface plate after vitro antibacterial assay. The surface plate of g) and j) *S. aureus*. h) The residual amount of bacterial on the superhydrophobic paper. i) The residual amount of bacterial on the surface plate after vitro antibacterial assay. k) The residual amount of bacterial on the raw paper. l) The residual amount of bacterial on the surface plate after vitro antibacterial assay.

online version, at <http://dx.doi.org/10.1016/j.cej.2018.04.023>.

## References

- [1] L. Peng, Y. Meng, H. Li, Facile fabrication of superhydrophobic paper with improved physical strength by a novel layer-by-layer assembly of polyelectrolytes and lignosulfonates-amine, *Cellulose* 23 (2016) 2073–2085.
- [2] H. Ogiwara, J. Xie, J. Okagaki, T. Saji, Simple method for preparing superhydrophobic paper: spray-deposited hydrophobic silica nanoparticle coatings exhibit high water-repellency and transparency, *Langmuir* 28 (2012) 4605–4608.
- [3] T. Arbatan, L. Zhang, X.Y. Fang, W. Shen, Cellulose nanofibers as binder for fabrication of superhydrophobic paper, *Chem. Eng. J.* 210 (2012) 74–79.
- [4] A.H. Grigoriou, Waste paper–wood composites bonded with isocyanate, *Wood Sci. Technol.* 37 (2003) 79–90.
- [5] S.A. Leonardi, M.A. Zanuttini, E.E. Miró, Catalytic paper made from ceramic fibres and natural ulexite. Application to diesel particulate removal, *Chem. Eng. J.* 317 (2017) 394–403.
- [6] T. Saito, M. Hirota, N. Tamura, S. Kimura, H. Fukuzumi, L. Heux, A. Isogai, Individualization of nano-sized plant cellulose fibrils by direct surface

- carboxylation using TEMPO catalyst under neutral conditions, *Biomacromolecules* 10 (2009) 1992–1996.
- [7] N. Holland, D. Holland, T. Helentjaris, K. Dhugga, B. Cazares, D. Delmer, A comparative analysis of the plant cellulose synthase (CesA) gene family, *Plant Physiol.* 123 (2000) 1313–1324.
- [8] S. Li, S. Zhang, X. Wang, Fabrication of superhydrophobic cellulose-based materials through a solution-immersion process, *Langmuir* 24 (2008) 5585–5590.
- [9] A. Lafuma, D. Quere, Superhydrophobic states, *Nat. Mater.* 2 (2003) 457–460.
- [10] S. Li, H. Li, X. Wang, Y. Song, Y. Liu, L. Jiang, D. Zhu, Super-hydrophobicity of large-area honeycomb-like aligned carbon nanotubes, *J. Phys. Chem. B* 106 (2002) 9274–9276.
- [11] X.M. Li, D. Reinhoudt, M. Crego-Calama, What do we need for a superhydrophobic surface? A review on the recent progress in the preparation of superhydrophobic surfaces, *Chem. Soc. Rev.* 36 (2007) 1350–1368.
- [12] B. Bhushan, Y.C. Jung, Natural and biomimetic artificial surfaces for superhydrophobicity, self-cleaning, low adhesion, and drag reduction, *Prog. Mater. Sci.* 1 (2011) 1–108.
- [13] D.K. Sarkar, M. Farzaneh, Superhydrophobic coatings with reduced ice adhesion, *J. Adhes. Sci. Technol.* 23 (2009) 1215.
- [14] S. Khorsand, K. Raeissi, F. Ashrafizadeh, M.A. Arenas, A. Conde, Corrosion behaviour of super-hydrophobic electrodeposited nickel–cobalt alloy film, *Appl. Surf. Sci.* 364 (2016) 349–357.
- [15] L. Wang, J. Yang, Y. Zhu, Z. Li, T. Shen, D.Q. Yang, An environment-friendly fabrication of superhydrophobic surfaces on steel and magnesium alloy, *Mater. Lett.* 171 (2016) 297–299.
- [16] X. Deng, L. Mammen, H.J. Butt, D. Vollmer, Candle soot as a template for a transparent robust superamphiphobic coating, *Science* 335 (2012) 67–70.
- [17] B. Qian, Z. Shen, Fabrication of superhydrophobic surfaces by dislocation-selective chemical etching on aluminum, copper, and zinc substrates, *Langmuir* 21 (2005) 9007–9009.
- [18] B. Balu, V. Breedveld, D.W. Hess, Fabrication of “roll-off” and “sticky” superhydrophobic cellulose surfaces via plasma processing, *Langmuir* 24 (2008) 4785–4790.
- [19] Y. Si, Z. Guo, Eco-friendly functionalized superhydrophobic recycled paper with enhanced flame-retardancy, *J. Colloid Interface Sci.* 477 (2016) 74–82.
- [20] S. Rezaei, I. Manoucheri, R. Moradian, B. Pourabbas, One-step chemical vapor deposition and modification of silica nanoparticles at the lowest possible temperature and superhydrophobic surface fabrication, *Chem. Eng. J.* 252 (2014) 11–16.
- [21] Y. Liu, X. Chen, J.H. Xin, Super-hydrophobic surfaces from a simple coating method: a bionic nanoengineering approach, *Nanotechnology* 17 (2006) 3259.
- [22] I.S. Bayer, D. Fragouli, A. Attanasio, B. Sorce, G. Bertoni, R. Brescia, R. Di Corato, T. Pellegrino, M. Kalyva, S. Sabella, P.P. Pompa, R. Cingolani, A. Athanassiou, Water-repellent cellulose fiber networks with multifunctional properties, *ACS Appl. Mater. Interface* 3 (2011) 4024–4031.
- [23] L.J. Zhang, C.F. Guerrero-Juarez, T. Hata, S.P. Bapat, R. Ramos, M.V. Plikus, R.L. Gallo, Dermal adipocytes protect against invasive staphylococcus aureus skin infection, *Science* 347 (2015) 67–71.
- [24] P. Li, Y.F. Poon, W. Li, H.Y. Zhu, S.H. Yeap, Y. Cao, X. Qi, C. Zhou, M. Lamrani, R.W. Beuerman, E.T. Kang, Y. Mu, C.M. Li, M.W. Chang, S.S. Leong, M.B. Chan-Park, A polycationic antimicrobial and biocompatible hydrogel with microbe membrane suctioning ability, *Nat. Mater.* 10 (2011) 149–156.
- [25] Q. Yang, M. Li, O.B. Spiller, T. Walsh, Balancing mcr-1 expression and bacterial survival is a delicate equilibrium between essential cellular defence mechanisms, *Nat. Commun.* 8 (2017) 2054.
- [26] K.J. Brobbey, J. Haapanen, M. Gunell, E. Eerola, M. Toivakka, J.J. Saarinen, One-step flame synthesis of silver nanoparticles for roll-to-roll production of anti-bacterial paper, *Appl. Surf. Sci.* 420 (2017) 558–565.
- [27] M.J. Nine, D.N.H. Tran, A. ElMekawy, D. Losic, Interlayer growth of borates for highly adhesive graphene coatings with enhanced abrasion resistance, fire-retardant and antibacterial ability, *Carbon* 117 (2017) 252–262.
- [28] Z.Q. Xu, M. Li, X. Li, X.M. Liu, F. Ma, S.L. Wu, K.W.K. Yeung, Y. Han, P.K. Chu, Antibacterial activity of silver doped titanate nanowires on Ti implants, *ACS Appl. Mater. Interfaces* 8 (2016) 16584–16594.
- [29] H. Bai, F. Walsh, B. Gludovatz, B. Delattre, C. Huang, Y. Chen, A. Tomsia, R. Ritchie, Bioinspired hydroxyapatite/Poly (methyl methacrylate) composite with a nacre-mimetic architecture by a bidirectional freezing method, *Adv. Mater.* 28 (2016) 50–56.
- [30] Y.G. Zhang, Y.J. Zhu, F. Chen, Ultralong hydroxyapatite nanowires synthesized by solvothermal treatment using a series of phosphate sodium salts, *Mater. Lett.* 144 (2015) 135–137.
- [31] J. Tian, H. Feng, L. Yan, M. Yu, H. Ouyang, H. Li, W. Jiang, Y.M. Jin, G. Zhu, Z. Li, Z.L. Wang, A self-powered sterilization system with both instant and sustainable anti-bacterial ability, *Nano Energy* 36 (2017) 241–249.
- [32] R.K. Ramesh, S.P.K. Chottanahalli, N.M. Madegowda, V.R. Rai, S. Ananda, Electrochemical synthesis of hierarchical flower-like hierarchical  $\text{In}_2\text{O}_3/\text{ZnO}$  nanocatalyst for textile industry effluent treatment, photo-voltaic, OH scavenging and anti-bacterial studies, *Catal. Commun.* 89 (2017) 25–28.
- [33] L. Vayssieres, Growth of arrayed nanorods and nanowires of ZnO from aqueous solutions, *Adv. Mater.* 15 (2003) 464–466.
- [34] H. Li, S. Yu, Three-level hierarchical superhydrophobic Cu–Zn coating on a steel substrate without chemical modification for self-cleaning property, *New J. Chem.* 41 (2017) 5436–5444.
- [35] A. Ultee, M.H.J. Bennik, R. Moezelaar, The phenolic hydroxyl group of carvacrol is essential for action against the food-borne pathogen *Bacillus cereus*, *Appl. Environ. Microbiol.* 68 (2002) 1561–1568.
- [36] G. Penel, G. Leroy, C. Rey, E. Bres, MicroRaman spectral study of the  $\text{PO}_4$  and  $\text{CO}_3$  vibrational modes in synthetic and biological apatites, *Calcified Tissue Int.* 63 (1998) 475–481.
- [37] L. Zhang, R. He, H.C. Gu, Oleic acid coating on the monodisperse magnetite nanoparticles, *Appl. Surf. Sci.* 253 (2006) 2611–2617.
- [38] G. Wen, Z.G. Guo, W.M. Liu, Biomimetic polymeric superhydrophobic surfaces and nanostructures: from fabrication to applications, *Nanoscale* 9 (2017) 3338–3366.
- [39] K. Krupa, A. Tonello, B.M. Shalaby, M. Fabert, G. Millot, S. Wabnitz, V. Couderc, Spatial beam self-cleaning in multimode fibres, *Nat. Photonics* 11 (2017) 237–241.
- [40] C. Cao, M. Ge, J. Huang, S. Li, S. Deng, S. Zhang, Z. Chen, K. Zhang, Y. Lai, Robust fluorine-free superhydrophobic PDMS–ormosil@ fabrics for highly effective self-cleaning and efficient oil–water separation, *J. Mater. Chem. A* 4 (2016) 12179–12187.
- [41] F. Guo, Q. Wen, Y. Peng, Z.G. Guo, Simple one-pot approach toward robust and boiling-water resistant superhydrophobic cotton fabric and the application in oil/water separation, *J. Mater. Chem. A* 5 (2017) 21866–21874.
- [42] J. Li, C. Xu, Y. Zhang, Robust superhydrophobic attapulgite coated polyurethane sponge for efficient immiscible oil/water mixture and emulsion separation, *J. Mater. Chem. A* 4 (2016) 15546–15553.
- [43] F. Wan, D.Q. Yang, E. Sacher, Repelling hot water from superhydrophobic surfaces based on carbon nanotubes, *J. Mater. Chem. A* 3 (2015) 16953–16960.
- [44] R. Sun, A. Nakajima, A. Fujishima, Photoinduced surface wettability conversion of  $\text{ZnO}$  and  $\text{TiO}_2$  thin films, *J. Phys. Chem. B* 105 (2001) 1984.
- [45] Z. Sun, T. Liao, K. Liu, L. Jiang, J.H. Kim, S.X. Dou, Robust superhydrophobicity of hierarchical  $\text{ZnO}$  hollow microspheres fabricated by two-step self-assembly, *Nano Res.* 6 (2013) 726–735.
- [46] J. Hou, Y. Gu, Y. Hu, Gigantic enhancement in response and reset time of  $\text{ZnO}$  UV nanosensor by utilizing Schottky contact and surface functionalization, *Appl. Phys. Lett.* 94 (2009) 191103.
- [47] W. Zhang, X. Lu, Z. Xin, C. Zhou, A self-cleaning polybenzoxazine/ $\text{TiO}_2$  surface with superhydrophobicity and superoleophilicity for oil/water separation, *Nanoscale* 7 (2015) 19476–19483.
- [48] M. Liu, J. Li, Y. Hou, Z. Guo, Inorganic adhesives for robust superwetting surfaces, *ACS Nano* 11 (2017) 1113–1119.
- [49] B. Chen, J. Qiu, E. Sakai, N. Kanazawa, R. Liang, H. Feng, Robust and superhydrophobic surface modification, *ACS Appl. Mater. Interfaces* 8 (2016) 17659–17667.
- [50] Y. Lu, S. Sathasivam, J. Song, C.R. Crick, C.J. Carmalt, I.P. Parkin, Robust self-cleaning surfaces that function when exposed to either air or oil, *Science* 347 (2015) 1132–1135.
- [51] H.S. Lim, J.H. Baek, K. Park, H. Shin, J. Kim, J. Sho, Multifunctional hybrid fabrics with thermally stable superhydrophobicity, *Adv. Mater.* 22 (2010) 2138–2141.
- [52] N.R. Chiou, C. Lu, J. Guan, L.J. Li, A.J. Epstein, Growth and alignment of poly-aniline nanofibres with superhydrophobic, superhydrophilic and other properties, *Nat. Nanotechnol.* 2 (2007) 354–357.
- [53] Z.Y. Wu, C. Li, H.W. Liang, J.F. Chen, S.H. Yu, Ultralight, flexible, and fire-resistant carbon nanofiber aerogels from bacterial cellulose, *Angew. Chem. Int. Ed.* 125 (2013) 2997–3001.
- [54] C. Mao, C. Liang, W. Luo, J. Bao, J. Shen, Preparation of lotus-leaf-like polystyrene micro- and nanostructure films and its blood compatibility, *J. Mater. Chem.* 19 (2009) 9025–9029.
- [55] T. Ishizaki, N. Saito, O. Takai, Correlation of cell adhesive behaviors on superhydrophobic, superhydrophilic, and micropatterned superhydrophobic/superhydrophilic surfaces to their surface chemistry, *Langmuir* 26 (2010) 8147–8154.
- [56] M. Spasova, N. Manolova, N. Markova, I. Rashkov, Superhydrophobic PVDF and PVDF–HFP nanofibrous mats with antibacterial and anti-biofouling properties, *Appl. Surf. Sci.* 363 (2016) 363–371.
- [57] O. Yamamoto, M. Hotta, J. Sawai, Influence of powder characteristic of  $\text{ZnO}$  on antibacterial activity, *J. Ceram. Soc. Jpn.* 106 (1998) 1007–1011.